Spin-phonon coupling and q-dependence of spin excitations and high-T_c superconductivity from band models

T. Jarlborg
DPMC, University of Geneva, 24 Quai Ernest-Ansermet, CH-1211 Geneva 4, Switzerland
(Received 5 March 2009; published 31 March 2009)

Spin-phonon coupling (SPC) has been shown to be compatible with many unusual properties of the high-T_c copper oxides. Parameters from *ab initio* band calculations for unit cells of La_2CuO_4 are used in a free-electron-like model in order to study the variation in coupling between spin waves and different phonons. Different SPC for different phonons can explain the "hour-glass" shape of the spin excitations. The model predicts larger q vectors at less doping and rather complex isotope shifts. A link between the SPC parameters and the parameters for superconductivity is proposed. Also the pseudogap depends on the efficiency of SPC, and it will interfere with superconductivity at low doping. Different contributions to the coupling parameters λ are discussed. It is argued that λ_{SPC} coming from the interaction between spin waves and O phonons can be strong enough to explain high T_c.

DOI: 10.1103/PhysRevB.79.094530 PACS number(s): 74.25.Jb, 74.20.Mn, 74.72.−h

I. INTRODUCTION

Several different families of high-T_c copper oxides exist with varying T_c but they have many things in common.[1] They are layered structures, where one or several rather flat CuO planes are separated by heavier elements, with two-dimensional (2D) electronic properties and very little interaction perpendicular to the layers. Angular resolved photoemission confirms that the band structure agrees well with calculations, where each CuO layer gives rise to a dispersive band along the planes with a barrel-like Fermi surface (FS) (or a FS "arc" when displayed in 1/4 of the Brillouin zone).[2–4] The Cu d states are the dominant electron states at the Fermi energy, E_F. The FS arc is not complete at low temperature, T, when it can only be observed in the diagonal direction ($k_x \approx k_y$).[5] Many measurements have revealed the existence of complex superstructures and pseudogaps surrounding E_F up to a temperature T^*, which is higher than T_c in underdoped systems. Phonons are closely interacting with the electronic states, as shown by the softening of some phonon branches at certain dopings,[6–8] by isotope effects on T^*, on T_c,[9] and on the width of the gap.[10] Stripelike regions with excitations of charge and spin modulations are seen in neutron-scattering experiments.[11] Noncommensurate q-dependent spin excitations deviate from the (0.5,0.5) point and move linearly with doping up to a saturation at $x \approx 0.12$.[12] Recent measurements on several cuprates reveal local-moment fluctuations and the underlying spin excitations have a characteristic "hour-glass-shaped" $(\bar{q}, \omega)$ dispersion even at nonsuperconducting compositions.[13–17]

Coupling between phonons and charge transfers as well as between phonon and spin waves has been proposed in relation to phonon softening and the mechanism for superconductivity.[18–20] *Ab initio* band calculations for supercells containing one-dimensional (1D) phonon and spin-wave modulations in the CuO bond direction ([1,0,0]) show large spin-phonon coupling (SPC) within the CuO plane.[18] This means that an antiferromagnetic (AFM) wave of the correct wavelength and phase is stronger when it coexists with the phonon. These results, in combination with 2D nearly free-electron (NFE)-like bands, have been used for modeling of many normal-state properties of the high-T_c materials.[21–23] Phonon softening, dynamical stripes, correlation between $\bar{q}$ and x, smearing of the nondiagonal part of the FS, and abrupt disappearance of the spin fluctuations at a certain T^* are possible consequences of SPC within a rather conventional band.[24]

Here, it is suggested that the characteristic spin dispersion can be understood in terms of SPC and that phonons promote a large λ_{sf} for spin fluctuations, and therefore SPC is important for the mechanism of superconductivity. The calculations consider SPC between spin waves and four different types of phonon distortions.

Section II describes the band calculations and how the resulting parameters for SPC are used in the NFE model. In Sec. III there is a discussion of the results for the spin excitations with comparisons to experiments. Section IV presents a connection between the parameters for SPC and the mechanisms for superconductivity.

II. BAND CALCULATIONS

Ab initio band calculations are made for long supercells of $La_{(2-x)}Ba_xCuO_4$ (LBCO), oriented along the CuO bond direction, where the virtual-crystal approximation (VCA) is applied to La sites to account for the doping. The calculations use the linear muffin-tin orbital (LMTO) method in the local spin-density approximation (LSDA), as has been described previously.[23] It is necessary to know the distortion amplitudes for the atoms (u, the distance from the equilibrium position) and the size of Cu moments (m) when calculations are made for phonons and spin waves, respectively. They can in principle be calculated in LSDA, but it is convenient to derive these quantities from experimental data. Measured[25,26] and calculated[27,28] phonon frequencies for zone-boundary phonons for $YBa_2Cu_3O_7$ (YBCO) agree well. Such values are also indicative for typical $\hbar\omega$ for each atomic character of the phonon density of states (DOS) in other copper oxides. Phonon energies and partial phonon DOS for each site i, calculated by Chen and Callaway[29] for

TABLE I. The four first lines: phonon distortion amplitudes, u/a_0, maximum $m(\mu_B)$, induced potential shifts, V_q^p (mRy), and exchange splitting, V_q^m (mRy) caused by spin waves ($\mu_B H = \pm 5$ mRy). All shifts/splittings refer to the maximal value on a Cu site, and they are determined in self-consistent LMTO calculations for supercells of length $8a_0$. Remaining lines: the partial characters of the phonon DOS, N_i, for different sites, i, as estimated from Ref. 29.

Wave	No phonon	pl-O_x	La_z	ap-O_z	Cu_x
u/a_0		0.014	0.021	0.013	0.020
m	0.09	0.15	0.14	0.12	0.10
V_q^p		15	2	5	3.5
V_q^m	8	12.5	12	10	8.5
$N_{\text{pl-O}}$		0.6	0.0	0.2	0.2
N_{La}		0.0	0.65	0.0	0.35
$N_{\text{ap-O}}$		0.35	0.0	0.65	0.0
N_{Cu}		0.2	0.2	0.0	0.6

Nd_2CuO_4 (NBCO), can be assumed to be representative for LBCO. From those results and measurements it can be deduced that the main La modes are at 10–20 meV, Cu at 20–30 meV, planar O near 50 ± 20 meV, and apical O at 60 ± 15 meV.[25,27,29] The reduction in the partial phonon DOS into single constants C_i from the figures in Ref. 29, shown in the last part of Table I, might seem to be subjective, but the qualitative results of the spin excitations will not depend on fine details of the phonon DOS. The force constants K_u are accessible in calculations as $K_u = d^2E/du^2$, where E is the total energy, or experimentally from the vibration frequency of a mass M, $K_u = M\omega^2$. Here they are defined from the site-dependent phonon energies, $\hbar\omega_i$, calculated for NBCO,[29] through the relations between ω and K_u for not too low T,

$$K_u^i = M_{\text{eff}}^i \omega_i^2 \tag{1}$$

and

$$u^2 = 3k_B T/K_u^i, \tag{2}$$

where the effective mass is given by $1/M_{\text{eff}} = \Sigma_i C_i/M_i$. The resulting u/a_0, where a_0 is the lattice constant, shown in Table I for $T \approx 120$ K (near T_c and T^*), compare well with experiment.[30] The force constants for other high-T_c cuprates, such as $YBa_2Cu_3O_7$, are not very different.[25,26]

An analogous description of the magnetic counterparts gives $K_m = d^2E/dm^2$ and $m^2 \approx k_B T/K_m$. Calculations for a short wave in $HgBa_2CuO_4$ (HBCO) resulted in magnetic moments on Cu of about $\sim 0.1\mu_B$.[22] Moments of about $0.1-0.15\mu_B$/Cu are obtained for LBCO if an AFM field of ± 5 mRy is applied on Cu sites in calculations for a cell of length $8a_0$, see Table I. The moments are larger for longer cells, in agreement with moments found within CuO layers in recent NMR measurements.[31] The *ab initio* calculations in HBCO show that K_m is sensitive to structural modifications, doping, and details of the LSDA scheme.[32] The exact values of K_m are not used in calculations here, but later it is assumed that they are small compared to the value of phonon force constant.

The calculated results for the maximal potential shifts (V_q^p on Cu) caused by phonons and by spin waves (V_q^m in the spin-polarized potential) for the four types of movements in the cell are shown in Table I, together with the result for V_q^m without phonons. These calculations consider distortions (and coexisting AFM spin waves) in cells extending $8a_0$ along $\bar{x}$, with displacements of La and apical O along $\bar{z}$, and Cu and planar O along $\bar{x}$. For the latter phonon there is a positive SPC when the nodes of the AFM waves are located at the "compressed" Cu sites (between the O atoms moving toward the Cu). Optimal SPC for displacements of out-of-plane atoms (La and apical O) occurs when these atoms move toward the CuO plane near the region of the AFM node. A modulation of apical O with the opposite phase will reduce V_q^m from 10 to below 8 mRy.

The LMTO results for a wave of length $8a_0$ are made for $k_B T \sim 10$ meV. Longer waves (for x closer to optimal doping) will have larger m at this temperature and correspond to about $0.2\mu_B$ on the Cu when the spins are coupled to plane-O modes. A Cu mode or involvement of no phonon would stir up about half as large moments at this temperature. Note that the matrix elements in λ's (see later) are made in the harmonic approximation, where the ratios between energy shifts and the amplitudes of the perturbations are constant.

The LMTO results calculated for waves of length $8a_0$ are rescaled to be valid for the longer waves at doping $x = 0.17$ ($12-13a_0$ in the model calculation) when V_q^p and V_q^m are larger by factors of ~ 1.1 and ~ 1.5, respectively, see Ref. 24. The total V_q^t can be summarized as

$$V_q^t = \sum_i (1.1V_{q,i}^p + 1.5V_{q,i}^m)C_i, \tag{3}$$

where i is the site index. The resulting V_q^t are 17, 18, 23, and 22 mRy at the energies centered around 17 (La), 27 (Cu), 48 (plane O), and 58 meV (apical O), respectively.

A calculation is also made for lower doping $x \approx 0.11$ when the wavelengths are longer and V_q are larger. Precise *ab initio* values are difficult to obtain because the requirement of long unit cells ($16a_0$ or more) makes the self-consistent convergence very tedious. By simple extrapolation and the use

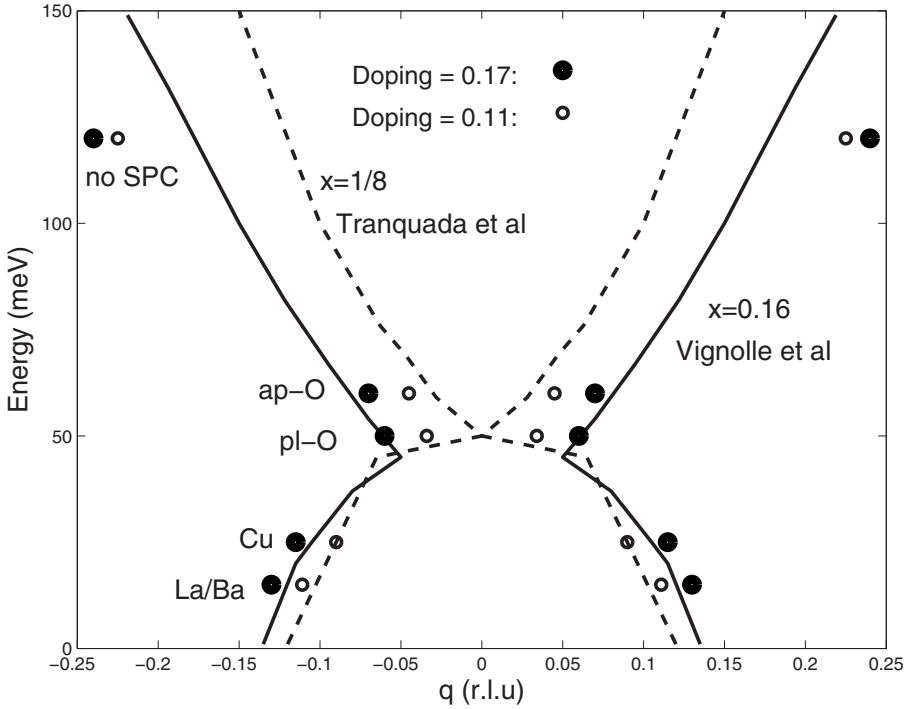

FIG. 1. Calculated $q-\hbar\omega$ relation from the 2D-NFE model for doping $x=0.17$ (filled circles) and 0.11 (open circles) with indication of the main SPC modes. Full line: approximate shape of the experimental dispersion as read from Fig. 3c in the work of Vignolle *et al.* (Ref. 15) for $La_{2-x}Sr_xCuO_4$ at $x=0.16$. Broken line: the dispersion for LBCO at $x=1/8$ as read from the data by Tranquada *et al.* (Ref. 14).

of the NFE model one can estimate that V_q^t are typically 40% larger at $x=0.11$. The spin part (V_q^m) is likely to grow faster as AFM stability approaches as $x\rightarrow 0$ and even more so for the waves which already have a large spin contribution such as the plane-O modes. The simple estimate with an overall increase of 40% makes V_q^t about 32, 31, 25, 23, and 12 mRy for ap-O, pl-O, Cu, La/Ba, and no phonon, respectively. As discussed later, spin waves at higher energy are not much dependent on phonons, and here it is assumed that $V_q^p=0$.

In a second step we use the parameters V_q^t in a 2D-NFE model.[24] The AFM spin arrangement on neighboring Cu along [1,0,0] in undoped LBCO corresponds to a potential perturbation, $V(\bar{x})=V_q^t \exp(-i\bar{Q}\cdot\bar{x})$ (and equivalently with $\bar{y}$ along [0,1,0]). The periodicity in real space is defined through the Cu-Cu distance, and a gap of size $2V_q^t$ appears at the zone boundary, at $\bar{Q}/2$. A further modulation ($\bar{q}$) of this order into 1D stripes perpendicular to $\bar{x}$ (or "checkerboards" in two dimensions along $\bar{x}$ and $\bar{y}$) is achieved by a multiplication of the potential by $\exp(i\bar{q}\cdot\bar{x})$, where $\bar{q}<\bar{Q}$. Totally, this makes $V(\bar{x})=V_q^t \exp(-i\bar{Q}_x\cdot\bar{x})$, where $\bar{Q}_x=\bar{Q}-\bar{q}$. The periodicity of this potential is now larger, and the gap moves away from $\bar{Q}/2$ to $(\bar{Q}-\bar{q})/2$. Magnetic side spots from the modulations would appear at $\bar{q}/2$ surrounding $\bar{Q}/2$. The main spots are caused by the underlying near-neighbor AFM correlation. A 3×3 eigenvalue problem with matrix elements $H_{11}=E-k_x^2-k_y^2$, $H_{22}=E-(k_x-Q_x)^2-k_y^2$, $H_{33}=E-k_x^2-(k_y-Q_y)^2$, $H_{12}=H_{13}=V_q^t$, and $H_{23}=0$ is solved. The effective mass of the NFE band is chosen so that the bandwidth from Γ to the M point is 0.3 Ry (when $V_q^t=0$). This makes the band dispersion near E_F quite close to the real band, and the NFE band is sufficient to demonstrate the effects of SPC. The model is entirely 2D (the DOS is constructed from a sum over all states in the plane), which is reasonable in view of the very small band dispersion along $\bar{k}_z$ of real band structures for the cuprates.[18]

III. SPIN EXCITATIONS

An important result of the 2D-NFE model is that it leads to a correlation between doping and the amplitude of V_q^t.[24] The reason is that the gap opens along $(k_x,0)$ and $(0,k_y)$ but not in the diagonal direction. Therefore, the dip in the total DOS (at which E_F should fall for optimal doping) will not appear at the same energy for small and large V_q even if the q vector is the same. But it could reappear at E_F if the q vector is allowed to change. This is why $\vec{q}$ will be different for different modes. The parameters in the calculations at 0.17 holes per Cu (which is close to x in Ref. 15) are summarized in Table I. The total V_q^t are obtained from Eq. (1). The calculations at $x=0.11$ (closer to the doping in Ref. 14) are based on larger V_q^t's, as explained above.

The results are shown in Fig. 1 together with experimental data from Refs. 14 and 15. The spectra are shaped like an hour glass with a "waist" at intermediate energy, which in the SPC model is because the strength of V_q^t differs with energy (no SPC would make $\vec{q}$ equal for all energies). The points below 70 meV are for the coupling to the four types of phonons. The general shape of the $q-\omega$ dependence and the amplitudes of q are similar as in the measurements, with the smallest q at about 0.05 for SPC dominated by O p phonons around 50 meV. The weaker SPC for La at low energy makes

TABLE II. Magnetic moments (m, μ_B/Cu) for two AFM spin waves along the [1,1,0] direction calculated for two unit-cell lengths with and without phonon distortions. Distortion amplitudes and magnetic fields as in Table I.

Wavelength	No phonon	pl-O_x	La_z	ap-O_z	Cu_x
$8\sqrt{2}a_0$	0.09	0.15	0.18	0.12	0.11
$4\sqrt{2}a_0$	0.06	0.09	0.08	0.08	0.07

q larger. The calculated results depend on the different parameters in the NFE model, so that a larger band mass leads to smaller amplitudes of q. If no mixing of the phonon modes (through the C_i coefficients) was made, it would increase the variations in q, even though the general hour-glass shape would remain.

Spin waves and phonons of the same frequency and q vector are closely connected for an optimal mechanism of SPC. Spin waves with higher frequency than the phonons cannot profit from this mechanism. Here it is assumed that spin waves with frequencies higher than the phonon frequencies are independent of lattice vibrations, whereby $V_q^p=0$. This "phonon-independent" result is put rather arbitrarily at $\hbar\omega\sim 120$ meV in Fig. 1, which is about twice the highest phonon frequency. The solution without SPC leads to a wave which is close to (or slightly shorter than) the cell in the LMTO calculation, so the factor 1.5 in Eq. (1) is reduced to ~ 1.0 for this (phonon-free) mode. Thus, the appropriate value of V_q^t is 8 mRy, with the solution at $q=0.24$, see Fig. 1. In contrast to the cases with SPC and larger V_q^t, this solution implies a very short wave, $4-5a_0$ only, where V_q^t might be reduced even more. This will, because of the self-consistent feedback between spin density and potential, lead toward a vanishing spin wave.[23]

Other high-energy solutions with small V_q^t exist for nonequal q vectors along x and y,[24] where the upper of two gaps corresponds to a doping close to 0.17. These solutions are found within some range of q, but the dips in the DOS are relatively weak. A satisfactory solution could be obtained for q_x and q_y near 0.145 and 0.11, respectively. The average of the two vectors, 0.13, is comparable to the wavelength in the LMTO calculation (where $V_q^m=8$ mRy). Two gaps remain in the DOS for larger separation of the two q vectors, but the dips are found at too high and too low dopings. The existence of this multitude of solutions indicates that large broadening and damping is expected at high energies. Such fluctuations are spread in energy and momentum, and they decay rapidly since they are not linked to the phonon spectrum.

However, there is a possibility for indirect SPC for high-energy spin excitations. As has been shown, slow movements of La/Ba along $\vec{z}$ lead to stronger spin waves. It can be imagined that rapid spin fluctuations, with different q vectors than that of the phonon, can be enhanced during the slow movement of the atoms. The details of such a mechanism are complicated and will not be investigated here. But it is not excluded that phonons will have some effects on spin waves also at high energy through a mechanism of indirect coupling.

Less doping will make the waves longer and the waist in the $\bar{q}-\hbar\omega$ diagram becomes narrower. The results for $x=0.11$ are shown by the open circles in Fig. 1. The band mass and the phonon energies are assumed to be the same as for $x=0.17$. The narrowing is relatively prominent for the O modes where the V_q are largest. But some narrowings are noticed for all points even at the highest E where spin waves are excited without direct coupling to phonons. Smaller q vectors at less doping are in agreement with observations in LBCO for $x=1/8$,[14] although the shifts are smaller than what is measured, see Fig. 1. Very small q vectors have been observed recently in lightly doped $La_{1.96}Sr_{0.04}CuO_4$,[33] but the spin modulation has turned from the parallel (the Cu-O bond) to the diagonal direction at this very low doping. Calculations for waves with q vectors along [1,1,0] cannot consider sufficiently long wavelengths to correspond to the low doping, but the results for short waves show that V_q for movements of oxygen atoms are larger than for movements of Cu. The magnetic moments on Cu for cells of lengths $8\sqrt{2}a_0$ and $4\sqrt{2}a_0$ along [1,1,0] are shown in Table II. The directions and the amplitudes of the distortions are as for the case with the q vectors along [1,0,0] (i.e., the distortions are no longer parallel to $\vec{q}$ for the plane-O and Cu modes). The plane-O mode has large AFM moment fluctuations, as for $\vec{q}$ along [1,0,0], but other modes have grown in importance compared to modulations along [1,0,0]. This is consistent with the observation by Matsuda *et al.*[33] of a much narrower low-energy part (in the range 15–20 meV) of the spin-excitation spectrum for very low-doped ($x\sim 0.04-0.05$) $La_{2-x}Sr_xCuO_4$. The correlation between strength of the SPC and wavelength is also evident in the results for modulation along the diagonal, as is shown in Table II by the consistently smaller m for the shortest cell.

According to the mechanism of SPC there is a possibility for increased AFM moment fluctuations at large T when the amplitude of u is increased. But the Fermi-Dirac occupation will catch up with this process and m will go down quickly near T^*.[23] This can lead to a narrower spin-excitation spectrum for increasing T before the disappearance of clear spin waves near T^*. A quite strong tendency for shorter q vectors for increasing T was reported by Matsuda *et al.*[33] at low energy and low doping. This appears to be stronger than the expected variation in SPC, but on the other hand, an extreme sensitivity is expected when the exchange enhancement diverges at such low doping. The exact behavior for T closer to T^* is hard to predict because of the rapid weakening of the spin waves in that T range.

Isotope shifts on the spin excitations have been proposed,[34] but no significant shift of energy due to exchange of O isotopes ($O^{16}\rightarrow O^{18}$) has been observed in LSCO.[35] This may seem surprising in view of the model for strong SPC if the phonon frequency $\omega\sim M^{-1/2}$. However, many intervened dependencies make isotope shifts compli-

TABLE III. Phonon energies (meV) and force constants (eV/Å^2) from experimental and calculated information (Refs. 25–29). Calculated electron-phonon coupling, λ_{ep}, and coupling constant, λ_{SPC}, for spin fluctuations mediated by phonons. The T_c's are estimated from the BCS formula.

Wave	pl-O_x	La_z	ap-O_z	Cu_x	Average	T_c
$\hbar\omega$	48	17	58	27	39	
K_u	12	5.5	14	6.5		
λ_{ep}	1.1	0.02	0.13	0.06	0.36	30
λ_{SPC}	0.78	0.68	0.47	0.38	0.60	95

cated here. For instance, the force constant for vibrations depend on several atoms and the use of an effective mass instead of the mass of one type of atoms will attenuate isotope shifts. Furthermore, heavier O isotopes should not only decrease the frequencies for the phonons and the coupled spin waves but they should also decrease u. At low temperature $u \sim M^{-1/4}$, which in the model for SPC will make V_q^t smaller. This implies two things. First, since SPC also predicts a sizeable phonon softening (by 15%–20%) (Ref. 23), there will be less softening for a heavy isotope when u is smaller, so that the downward isotope shift of ω is reduced. Second, smaller u and V_q^t will move the pseudogap toward lower energy, away from E_F. The SPC at the original $\vec{q}$ will no longer be supported if the gap is not at E_F, but other shorter q vectors will move in and restore a pseudogap at E_F (It is assumed that the doping is unchanged by isotope shifts.) Since SPC is a bit weaker for shorter waves, it will again renormalize V_q^t, $\vec{q}$, and u to lower values, and in the end there will be less phonon softening. This is a complicated self-consistent process and a quantitative prediction of the total reduction will be uncertain, but all effects tend to reduce the original isotope shift.

The possibility of indirect SPC may cause even more complicated isotope shifts, especially for changes in the heavy La/Ba atoms. The associated phonon frequencies are low, and the promotion of fast spin waves can be reduced if the distortion amplitudes of La/Ba are reduced through the change in isotopes. The high-energy excitations show little structure and evidence of isotope shifts from indirect SPC might be seen in the linewidths more than in the $q-\omega$ characteristics.

IV. SUPERCONDUCTIVITY

Undoped cuprates are generally stable AFM insulators. The exchange enhancement for spin waves in doped cuprates is moderately large in the absence of phonons, and as has been shown, it becomes peaked by the interaction with phonon distortions, especially at low doping. This unusual mechanism can be translated into a large *spin-polarized* contribution to the phonon deformation potential, which therefore has to be associated with λ_{sf} for AFM spin fluctuations. This can work in two ways. Many phonon modes are excited at a certain T, and a spin fluctuation can profit from the SPC to the available modes. A calculation of λ_{sf} can in this case be done without the phonon excitation but with the lattice distortion taken into account. The second mechanism is when the virtual excitations involve the phonon and the spin fluctuation together. The coupling constant for such a process, denoted by λ_{SPC}, is estimated later from the change in spin-polarized potential when an atom is displaced by Δu. A third coupling constant, λ_{ep}, is for conventional electron-phonon coupling. It turns out that the ingredients for all of these coupling constants are related to the same V_q parameters for phonons and spin excitations as determined above. Thus, there is a link between the key parameters for spin excitations and theories for superconductivity. For instance, V_q^p corresponds to the monopolar matrix element in electron-phonon coupling, λ_{ph}. The good agreement between the calculated spin excitations and experiment suggests that the calculated V_q's are of the correct order. Thus, on the basis of the band results obtained above, we consider contributions from pure phonons, from spin fluctuations coupled to phonons, and from independent spin fluctuations in estimations of λ and T_c.

Assume first that T_c depends exclusively on (harmonic) phonons without SPC. The rigid muffin-tin approximation (RMTA) leads to a simple estimate of $\lambda = NI_u^2/K_u$, where N is the DOS at E_F and I_u is the dipolar matrix element for the deformation potential,

$$I_u = \int \Psi^*(r) dV(r)/dr \Psi(r) d^3r = \langle dV/dr \rangle \tag{4}$$

(the integration is over the unit cell).[36] Ionic layered materials such as the cuprates have large monopolar contributions to I_u,

$$I_u = \langle \Delta V(r)/\Delta u \rangle \approx \Delta V^p/\Delta u, \tag{5}$$

where the last simplification is done if $\Delta V(r)$ is nearly constant within the contributing volume, i.e., for a rigid shift of the potential within one Cu.[37] This matrix element is the first-order change in the energy at E_F, which in the NFE model is equivalent to $V_q^p/\Delta u$. With $N \approx 0.9$(eV Cu spin)$^{-1}$ from the DOS near optimal doping (when the pseudogap is not much developed), ΔV^p from Table I, the K values from Table III, and with $a_0 = 3.78$ Å, this makes an average (averaged over the number of sites per cell) of $\lambda_{ph} \approx 0.36$. The plane-O phonon alone would make $\lambda_{ph} \approx 1.12$. This is in qualitative agreement with a recent calculation of the total (Brillouin zone averaged) λ_{ph} for LSCO of 0.4 where the electron-phonon matrix elements are "by far the largest" for the breathing modes,[38] which corresponds to the plane-O mode here. A similar calculation for YBCO gives an even smaller total $\lambda_{ph} \approx 0.2$.[39] The conclusion of these two works

is that λ_{ph} alone cannot explain the observed "kink" in the band dispersion close to E_F. This result (and a too low T_c) suggests that spin fluctuations are important for the kink and high T_c. Here, from the BCS formula $k_B T_c = 1.13\hbar\omega \exp(-1/\lambda)$,[40] T_c will be of the order 30 K for a site-averaged $\hbar\omega$ of 39 meV when strong-coupling effects and Coulomb repulsion are ignored. Smaller λ_{ph} are obtained for shorter waves (i.e., larger doping), as for HBCO,[22,24] and probably at very low doping when the pseudogap makes N small.

Next we consider spin fluctuations induced by phonons through SPC. Phonons are emitted and absorbed by the electrons as before but with the difference that the change in potential is now in the spin-polarized part. Such deformation potentials can be much larger than the conventional nonpolarized deformation potential for a system such as this since AFM fluctuations are strong at underdoping. Probably AFM order could even be stable if the lattice distortions were static and large. In contrast, AFM fluctuations would be rather weak in the absence phonons, in particular at overdoping. The spin-polarized $\Delta V^m(r)$ is essentially monopolar for modulations with long wavelengths with contributions mainly coming from Cu sites and is of the same order as ΔV^p for O modes (see Table I). The SPC analog to λ_{ph} can be estimated on the same level of approximation, $\lambda_{SPC} = NI_m^2/K_{SPC}$, where

$$I_m = \langle \Delta V^m(r)/\Delta u \rangle \approx V_q^m/\Delta u. \tag{6}$$

The quantity $\Delta V^m/\Delta u$ is constant in the harmonic approximation and can be estimated from the results shown in the tables. For instance, for the plane-O mode at 120 K, u is $0.014a_0$, m is about $0.15\mu_B$/Cu, and $V_m \approx 13$ mRy. The force constants K_{SPC} should be modified so that the total energy in d^2E/du^2 includes also the energy needed to create the spin wave (K_m). This is difficult to calculate because the total energy for spin fluctuations goes to zero near the singularity for diverging exchange enhancement, i.e., exactly for the interesting case of SPC. But some experimental facts are useful. For example, phonons in the energy range of oxygen modes can be ~20% softer in the doped high-T_c materials.[8] This is an indication of a negative K_m. Phonon softening and a negative contribution from K_m have been estimated for a coexisting phonon and spin wave.[23] By assuming zero energy from the spin wave for all modes ($K_m \approx 0$), this gives $\lambda_{SPC} \approx 0.6$ (and $T_c \approx 95$ K in BCS). The results are summarized in Table III. The contribution from different modes are not so different as in the case with λ_{ph}, but plane-O is still strongest. If no phonon softening exists for La and Cu modes, then K_m could be positive and perhaps large for such modes. If, in an extreme case, it is assumed that La and Cu modes have $K_m \gg 0$, so that such modes give zero contribution to λ_{SPC}, then λ_{SPC} will be reduced to 0.35.

The third possibility, a pure λ_{sf} without simultaneous excitations of phonons, (but calculated for lattices with phonon distortions), should be available from[41]

$$\lambda_{sf} = N\langle dV_m/dm \rangle^2/K_m. \tag{7}$$

The matrix element in the numerator dV_m/dm can be large near the AFM instability. It can increase with T because of the increasing distortion amplitudes of the existing phonons up to $T \approx T^*$. As was noted before, K_m is small for O distortions, and it will go down for increasing $u(T)$. But K_m is difficult to calculate, and corrections to the LDSA are needed.[32] Therefore, no calculated values of λ_{sf} for LBCO are presented here. A calculation including LSDA corrections for the shortest possible wave in HBCO with half-breathing distortions led to $K_m \approx 0.7$ eV$/\mu_B^2$ (i.e., no phonon softening) and a λ_{sf} of about 0.5.[32]

Clearly, these estimates are very approximate and should not be used for quantitative conclusions. But the point is that the order of magnitude is large enough for being interesting for high T_c. It is not clear if the total λ can be a combination of the three different mechanisms. However, the spin enhancement is sensitive to doping and it is likely that λ_{SPC} and λ_{sf} increase faster than λ_{ph} when the doping goes down. Many other facts suggest that λ_{SPC} could be larger. For instance, in addition to being larger for longer waves at less doping, it can also increase because of larger u through a "feedback" mechanism from SPC. The calculations are made for pure modes with one atom at the time, while hybridization in real phonons could make the deformation potentials stronger. Finally, as was indicated, probable corrections to LSDA are needed for realistic values. Such corrections tend to increase the exchange enhancement for AFM fluctuations.[32]

The SPC and spin fluctuations become very large at underdoping when the wave modulations are longest, so N (and λ) are reduced because of the pseudogap, and hence the pseudogap competes with superconductivity. Other reasons for competition between superconductivity and pseudogap have been proposed.[42,43] On the overdoped side λ is reduced because of a smaller ΔV, and $T_c \to 0$. Another reason for vanishing T_c at larger doping is that the wavelength for phonons and SPC will be too short to fit within the lattice. In addition, signs of weak ferromagnetic order have been seen in calculations for LBCO with clustering of dopants.[44] The different limitations at extreme dopings leave out a range of intermediate doping for optimal conditions for large λ's and high T_c.

V. CONCLUSION

These calculations suggest that the hour-glass-shaped dispersion of the spin-wave spectrum is a consequence of different degrees of SPC for different phonon modes. The "half-breathing" O-mode in the midpart of the phonon spectrum is found to be the most efficient one, which explains the waist in the spin-wave dispersion. The amplitude of the q vectors agree reasonably with experiments, which means that the amplitude of the parameters in the NFE model is of the correct order. These parameters are derived from results of *ab initio* calculations, but many assumptions and approximations are made. On the other hand, if the SPC-NFE model were used to fit the experimental data, it would give V_q parameters not too far from what is shown here. Moreover, other normal-state properties fit surprisingly well with the SPC-NFE simulation based on these parameters. Therefore, since it can be argued that the parameters are closely related to parameters for electron-phonon coupling and spin fluctua-

tions, there is a possible link between spin excitations and superconductivity. One important fact is that spin fluctuations may become peaked through the interaction with phonons, in particular at low doping. This makes spin fluctuations largely responsible for the pseudogap at low doping but also for the mechanism of superconductivity. The parameters for SPC are sufficiently large for high T_c at intermediate doping when the pseudogap is not much developed. Isotope effects will normally show up in both frequency and q dependencies, but many coincidences in the mechanism for SPC make them much reduced. There is no reason why they should cancel exactly, and it would be useful to pursue precise experiments where fine effects from phonons and isotope shifts can be seen in spin excitations.

ACKNOWLEDGMENT

I am grateful to B. Barbiellini and C. Berthod for useful discussions.

[1] T. Timusk and B. Statt, Rep. Prog. Phys. **62**, 61 (1999).
[2] A. Damascelli, Z.-X. Shen, and Z. Hussain, Rev. Mod. Phys. **75**, 473 (2003), and references therein.
[3] S. Sahrakorpi, M. Lindroos, R. S. Markiewicz, and A. Bansil, Phys. Rev. Lett. **95**, 157601 (2005).
[4] W. E. Pickett, Rev. Mod. Phys. **61**, 433 (1989).
[5] M. R. Norman, H. Ding, M. Randeria, J. C. Campuzano, T. Yokoya, T. Takeuchi, T. Takahashi, T. Mochiku, K. Kadowski, P. Guptasarma, and D. G. Hinks, Nature (London) **392**, 157 (1998).
[6] H. Uchiyama, A. Q. R. Baron, S. Tsutsui, Y. Tanaka, W. Z. Hu, A. Yamamoto, S. Tajima, and Y. Endoh, Phys. Rev. Lett. **92**, 197005 (2004).
[7] L. Pintschovius and M. Braden, Phys. Rev. B **60**, R15039 (1999).
[8] T. Fukuda, J. Mizuki, K. Ikeuchi, K. Yamada, A. Q. R. Baron, and S. Tsutsui, Phys. Rev. B **71**, 060501(R) (2005).
[9] D. Rubio Temprano, J. Mesot, S. Janssen, K. Conder, A. Furrer, A. Sokolov, V. Trounov, S. M. Kazakov, J. Karpinski, and K. A. Muller, Eur. Phys. J. B **19**, 5 (2001).
[10] G.-H. Gweon, T. Sasagawa, S. Y. Zhou, J. Graf, H. Takagi, D.-H. Lee, and A. Lanzara, Nature (London) **430**, 187 (2004).
[11] J. M. Tranquada, B. J. Sternlieb, J. D. Axe, Y. Nakamura, and S. Uchida, Nature (London) **375**, 561 (1995).
[12] K. Yamada, C. H. Lee, K. Kurahashi, J. Wada, S. Wakimoto, S. Ueki, H. Kimura, Y. Endoh, S. Hosoya, G. Shirane, R. J. Birgeneau, M. Greven, M. A. Kastner, and Y. J. Kim, Phys. Rev. B **57**, 6165 (1998).
[13] S. M. Hayden, H. A. Mook, P. Dai, T. G. Perring, and F. Doğan, Nature (London) **429**, 531 (2004).
[14] J. M. Tranquada, H. Woo, T. G. Perring, H. Goka, G. D. Gu, G. Xu, M. Fujita, and K. Yamada, Nature (London) **429**, 534 (2004).
[15] B. Vignolle, S. M. Hayden, D. F. McMorrow, H. M. Rönnow, B. Lake, and T. G. Perring, Nat. Phys. **3**, 163 (2007).
[16] D. Reznik, J.-P. Ismer, I. Eremin, L. Pintschovius, T. Wolf, M. Arai, Y. Endoh, T. Masui, and S. Tajima, Phys. Rev. B **78**, 132503 (2008).
[17] G. Xu, G. D. Gu, M. Hucker, B. Fauque, T. G. Perring, L. P. Regnault, and J. M. Tranquada, arXiv:0902.2802 (unpublished).
[18] T. Jarlborg, Phys. Rev. B **64**, 060507(R) (2001).
[19] M. Tachiki, M. Machida, and T. Egami, Phys. Rev. B **67**, 174506 (2003).
[20] P. Piekarz and T. Egami, Phys. Rev. B **72**, 054530 (2005).
[21] T. Jarlborg, Phys. Lett. A **295**, 154 (2002).
[22] T. Jarlborg, Phys. Rev. B **68**, 172501 (2003).
[23] T. Jarlborg, Physica C **454**, 5 (2007).
[24] T. Jarlborg, Phys. Rev. B **76**, 140504(R) (2007).
[25] C. Thomsen and M. Cardona, in *Physical Properties of High-Temperature Superconductors*, edited by D. M. Ginsberg (World Scientific, Singapore, 1989), p. 409.
[26] J. Humlicek, A. P. Litvinchuk, W. Kress, B. Lederle, C. Thomsen, M. Cardona, H. U. Habenmeier, I. E. Trofimov, and W. König, Physica C **206**, 345 (1993).
[27] R. E. Cohen, W. E. Pickett, and H. Krakauer, Phys. Rev. Lett. **64**, 2575 (1990).
[28] O. K. Andersen, A. I. Liechtenstein, O. Rodriguez, I. I. Mazin, O. Jepsen, V. P. Antropov, O. Gunnarsson, and S. Gopalan, Physica C **185-189**, 147 (1991).
[29] H. Chen and J. Callaway, Phys. Rev. B **46**, 14321 (1992).
[30] N. L. Saini, A. Lanzara, H. Oyanagi, H. Yamaguchi, K. Oka, T. Ito, and A. Bianconi, Phys. Rev. B **55**, 12759 (1997).
[31] Y. Kitaoka, H. Mukuda, and S. Shimizu, arXiv:0902.1381 (unpublished).
[32] T. Jarlborg, J. Phys.: Condens. Matter **16**, L173 (2004).
[33] M. Matsuda, M. Fujita, S. Wakimoto, J. A. Fernandez-Baca, J. M. Tranquada, and K. Yamada, Phys. Rev. Lett. **101**, 197001 (2008).
[34] I. Eremin, O. Kamaev, and M. V. Eremin, Phys. Rev. B **69**, 094517 (2004).
[35] S. Pailhes, P. Bourges, Y. Sidis, C. Bernhard, B. Keimer, C. T. Lin, and J. L. Tallon, Phys. Rev. B **71**, 220507(R) (2005).
[36] G. D. Gaspari and B. L. Gyorffy, Phys. Rev. Lett. **28**, 801 (1972).
[37] T. Jarlborg, Helv. Phys. Acta **61**, 421 (1988).
[38] F. Giustino, M. L. Cohen, and S. G. Louie, Nature (London) **452**, 975 (2008).
[39] R. Heid, K.-P. Bohnen, R. Zeyher, and D. Manske, Phys. Rev. Lett. **100**, 137001 (2008).
[40] J. Bardeen, L. N. Cooper, and J. R. Schrieffer, Phys. Rev. **108**, 1175 (1957).
[41] T. Jarlborg, Physica C **385**, 513 (2003).
[42] R. Zeyher and A. Greco, Phys. Status Solidi B **236**, 343 (2003).
[43] V. Hinkov, P. Bourges, S. Pailhés, Y. Sidis, A. Ivanov, C. D. Frost, T. G. Perring, C. T. Lin, D. P. Chen, and B. Keimer, Nat. Phys. **3**, 780 (2007).
[44] B. Barbiellini and T. Jarlborg, Phys. Rev. Lett. **101**, 157002 (2008).